HHS Public Access

Author manuscript

Magn Reson Med. Author manuscript; available in PMC 2016 February 07.

Published in final edited form as:

Magn Reson Med. 2015 July ; 74(1): 249–259. doi:10.1002/mrm.25401.

Multiparametric MRI Assessment of Human Articular Cartilage Degeneration: Correlation with Quantitative Histology and Mechanical Properties

Jari Rautiainen, MSc (Tech.)[1,2,3], **Mikko J. Nissi, PhD**[3,4], **Elli-Noora Salo**[5], **Virpi Tiitu, PhD**[6], **Mikko A.J. Finnilä, MHSc**[7], **Olli-Matti Aho, MD**[8], **Simo Saarakkala, PhD**[2,5,7], **Petri Lehenkari, MD, PhD**[8], **Jutta Ellermann, MD, PhD**[4], and **Miika T. Nieminen, PhD**[1,5]

[1]Department of Diagnostic Radiology, University of Oulu, Oulu, Finland [2]Medical Research Center Oulu, University of Oulu, Oulu, Finland [3]Department of Applied Physics, University of Eastern Finland, Kuopio, Finland [4]Center for Magnetic Resonance Research, Departments of Radiology and Orthopaedic Surgery, University of Minnesota, Minneapolis, Minnesota [5]Department of Diagnostic Radiology, Oulu University Hospital, Oulu, Finland [6]Institute of Biomedicine, Anatomy, University of Eastern Finland, Kuopio, Finland [7]Department of Medical Technology, University of Oulu, Oulu, Finland [8]Department of Anatomy and Cell Biology, University of Oulu, Oulu, Finland

Abstract

Purpose—To evaluate the sensitivity of quantitative MRI techniques (T_1, $T_{1,Gd}$, T_2, continous wave (CW) $T_{1\rho}$ dispersion, adiabatic $T_{1\rho}$, adiabatic $T_{2\rho}$, RAFF and inversion-prepared magnetization transfer (MT)) for assessment of human articular cartilage with varying degrees of natural degeneration.

Methods—Osteochondral samples ($n = 14$) were obtained from the tibial plateaus of patients undergoing total knee replacement. MRI of the specimens was performed at 9.4 T and the relaxation time maps were evaluated in the cartilage zones. For reference, quantitative histology, OARSI grading and biomechanical measurements were performed and correlated with MRI findings.

Results—All MRI parameters, except $T_{1,Gd}$, showed statistically significant differences in tangential and full-thickness ROIs between early and advanced osteoarthritis (OA) groups, as classified by OARSI grading. CW-$T_{1\rho}$ showed significant dispersion in all ROIs and featured classical laminar structure of cartilage with spin-lock powers below 1000 Hz. Adiabatic $T_{1\rho}$, $T_{2\rho}$, CW-$T_{1\rho}$, MT and RAFF correlated strongly with OARSI grade and biomechanical parameters.

Conclusion—MRI parameters were able to differentiate between early and advanced OA. Furthermore, rotating frame methods, namely adiabatic $T_{1\rho}$, adiabatic $T_{2\rho}$, CW-$T_{1\rho}$ and RAFF, as well as MT experiment correlated strongly with biomechanical parameters and OARSI grade, suggesting high sensitivity of the parameters for cartilage degeneration.

Corresponding author: Name: Jari Rautiainen, Mailing address: Department of Applied Physics, University of Eastern Finland, P. O. Box 1627, FI-70211 Kuopio, Finland, Telephone number: +358 40 355 3725, Fax number: +358 17 162585, jari.rautiainen@uef.fi.

Keywords

Quantitative MRI; osteoarthritis; cartilage; human; rotating frame relaxation

Introduction

Progressive degeneration of articular cartilage is typical in osteoarthritis (OA) (1, 2). At the early stage of the disease cartilage macromolecules are affected, the amount of proteoglycans (PG) decreases, water content of the cartilage increases and collagen fibril network is disrupted (1, 2). Also the mechanical properties of cartilage are compromised. As the disease advances, fibrillation occurs at the surface of the cartilage and ultimately leads to complete loss of the tissue due to cartilage thinning. The goal of OA diagnostics is to detect OA changes at the molecular level before irreversible tissue damage occurs. However, this is difficult to achieve with plain radiography, arthroscopy or conventional MRI.

Morphological changes in articular cartilage can be indirectly evaluated using quantitative MR relaxometry (3, 4). Previously, an increase in T_2 relaxation time has been linked to cartilage degeneration (5, 6), specifically to disorganization of the collagen network and increased tissue water content while T_1 relaxation time mapping -based delayed gadolinium (Gd) Enhanced MRI of Cartilage (dGEMRIC) has been used for assessment of the PG content of cartilage (6–8). Native T_1 relaxation time without contrast agents has not been extensively studied in cartilage, but rather as an additional step in dGEMRIC. T_1 has been reported to be sensitive to the water content in cartilage (9). Magnetization transfer (MT) methods probe the interactions of bound and free water pools and in cartilage, the observed reduction of signal from mobile protons due to off-resonance irradiation has been mainly associated to collagen (10).

$T_{1\rho}$ and $T_{2\rho}$, the longitudinal and transverse relaxation time parameters in the rotating frame of reference (RFR) enable assessment of slow molecular motions in the biological tissues probing magnetic field fluctuations close to effective field, in the kHz range (11). The $T_{1\rho}$ and $T_{2\rho}$ measurements can be implemented by spin-locking the magnetization with continuous wave (CW) radiofrequency (RF) irradiation or with amplitude and frequency modulated adiabatic hyperbolic secant (HSn, n = 1, 4, 8) pulse trains (12, 15, 16). Relaxation dispersion can be investigated by measuring $T_{1\rho}$ with multiple spin-locking amplitudes with CW-pulses or using different modulation functions with HSn pulses (14–17). Relaxation along a fictitious field (RAFF) is a low RF power RFR technique (18) that employs frequency modulated pulses that violate the adiabatic condition. Such pulses create a large fictitious field in so called second rotating frame creating measurable contrast in tissue (18).

Relationship between PG loss and increased T1ρ in CW-$T_{1\rho}$ imaging of cartilage has been found *in vitro* and *in vivo* (19–22). In addition, adiabatic $T_{1\rho}$, adiabatic $T_{2\rho}$ and RAFF were found promising in detection of cartilage degeneration in recent studies with animal models of OA (17, 23). In this study, parametric MRI imaging was conducted *in vitro* for human articular cartilage specimens with varying degrees of degeneration. Aforementioned RFR-techniques, MT, T_2-mapping and dGEMRIC methods were used and compared with biomechanical and histological reference methods. The specific aims of the study were to

identify which of the methods are sensitive to natural degeneration of human articular cartilage, how they reflect the properties of the tissue as determined by the reference methods, and how they compare to one another.

Methods

Sample preparation

Osteochondral plugs (n = 14) of 6 mm in diameter from human tibial plateaus were extracted from patients undergoing total knee arthroplasty (TKA). The samples were frozen at −20 °C. Prior to MR imaging, samples were thawed to room temperature in phosphate buffered saline (PBS) and then placed inside a Teflon test tube filled with perfluoropolyether to minimize susceptibility effects due to tissue-air interfaces and for ^{1}H signal-free background. The experiments were approved by the Ethical Committee of the Northern Ostrobothnia Hospital District, Oulu, Finland (191/2000).

Magnetic resonance imaging

Magnetic resonance imaging of the samples was performed at 9.4 T (Oxford 400 NMR vertical magnet, Oxford instruments Plc, Witney, UK) with a 19 mm quadrature RF volume transceiver (RAPID Biomedical GmbH, Rimpar, Germany) and Varian Direct Drive console (Varian Inc. Palo Alto, CA, USA) (24). The normal to the cartilage surface was set parallel to the B_0 field to control for the sample orientation. In all experiments, magnetization preparation (MP) block for contrast generation was coupled to a fast spin echo (FSE) readout. The MP block was modified for measurement of the following relaxation parameters: adiabatic $T_{1\rho}$ (25), adiabatic $T_{2\rho}$ (26), CW-$T_{1\rho}$ (12) with spin-lock frequencies of 125, 250, 500 and 1000 Hz, RAFF (20) and inversion prepared MT experiment measuring T_1 during off-resonance saturation (T_{1sat}) (27). In addition, T_2 was measured with spin echo and adiabatic double-echo (DE) (28) techniques. T_1 mapping was performed with saturation recovery FSE sequence before and after 24 hour immersion of the specimens in 1 mM Gd-DTPA^{2-} (Magnevist™, Bayer Healthcare, Montville, NJ, USA) ($T_{1,Gd}$). Measurement parameters for different MP methods and readout are summarized in Table 1.

Reference methods

Indentation testing with a plane-ended intender of 1 mm in diameter was performed for determination of the mechanical properties of the cartilage (29). Prior to mechanical testing, the thickness of the cartilage was measured with a high-resolution ultra-sound system (30). Equilibrium elastic modulus was obtained from step-wise relaxation tests (4x5 % step, 15 min relaxation after each step). Dynamic modulus was determined from sinusoidal tests (1 Hz frequency, amplitude of 1% of cartilage thickness) (30).

Histological sections were prepared for digital densitometry (DD), polarized light microscopy (PLM) and semi-quantitative histological grading. For DD and histological grading, 3 μm thick microscopic sections were stained with Safranin-O which binds stoichiometrically to the glycosaminoglycan side chains of the PGs. The obtained optical density (absorbance) from DD-measurements is linearly proportional to the PG content of the cartilage (31). Safranin-O stained sections were histologically graded by three observers

(V.T., M.A.J.F, O-M.A.) according to the Osteoarthritis Research Society International (OARSI) grading system (scale 0–6, zero indicating normal healthy cartilage) (32). PLM measurements were done on 5 μm thick unstained sections for determination of parallelism index of collagen fibril in the samples which is defined from the Stokes parameters (33). Parallelism index is an indicator for collagen fibril anisotropy; 1 indicates fibrils running parallel to each other and 0 indicates random arrangement. For all analyses, an average of three sections per sample was used. Furthermore, OARSI grades were calculated as an average of three observers.

Fourier transform infrared imaging (FTIRI) was conducted using Hyperion 3000 FTIRI Microscope (Bruker Inc, Germany). The acquired spectral resolution and the pixel size were 4 cm^{-1} and 25 μm, respectively. The spectral region of 950–1720 μm^{-1} was analyzed (34, 35). An offset baseline correction was performed for all spectra prior to analysis. Collagen content was estimated by integrating over the area of the amide I absorbance peak (1585–1720 μm^{-1}) and PG content similarly by integrating over the carbohydrate region (985–1140 μm^{-1}) (34, 35).

The total water content of the cartilage in the samples was determined biochemically. The articular cartilage was detached from the bone and the wet weight of the samples was measured three times and averaged, followed by freeze-drying. After lyophilization, the dry weight of the samples was determined. The water content was obtained as (1 – dry/wet weight)*100 % (30).

Data analysis

Samples were divided into two groups according to OARSI grading. The samples with OARSI grade less than 1.5 were labeled as early OA group ($n = 5$) and samples with OARSI grade higher than 1.5 as advanced OA group ($n = 9$) (36). MRI data was fitted to mono-exponential equation on a pixel-by-pixel basis for calculation of T_1, T_2, $T_{1\rho}$ and $T_{2\rho}$ relaxation time maps, and a mono-exponential fit with steady-state was used for RAFF and MT. For ROI analysis of the relaxation time maps, cartilage was divided to three zones: tangential, transitional and radial ROIs. In the early OA group, cartilage zones were segmented from T_2-maps using the laminar appearance as guide (37, 38). In the advanced OA group, thicknesses of the cartilage zones were taken as 5 %, 20 % and 75 %, respectively (38). Furthermore, a full-thickness ROI was also included into the analysis. For each ROI, average relaxation time ± standard deviation was calculated. The thicknesses of the full-thickness ROIs were compared against the thicknesses derived from microscopy images to avoid inclusion of residual PBS from top of the surface of the cartilage in the ROI. In addition, full-thickness cartilage ROIs were used to create mean depth-wise profiles of MRI relaxation parameters, which were linearly interpolated to normalized length of 10 points to allow depth-wise comparison. Similarly, normalized depth-wise profiles were calculated from DD, PLM and FTIR data. All data and ROI analysis was performed using in-house software and Aedes (http://aedes.uef.fi) in MATLAB (MATLAB R2010a, MathWorks, Natick, MA, USA).

Statistical analyses

The Mann-Whitney U-test was used for evaluating differences in MRI parameters and reference methods between early OA and advanced OA groups. A P-value < 0.05 was considered as statistically significant. Pearson correlation coefficients were calculated for pooled data of both sample groups between average MRI relaxation time values in full-thickness ROIs and bulk values of equilibrium and dynamic moduli, water content, optical density, parallelism index, OARSI grade, amide I region absorption and carbohydrate region absorption. In addition, the correlation between biomechanical parameters (equilibrium and dynamic moduli) and other reference methods was investigated. Receiver operating characteristics (ROC) analysis was performed for MRI parameters for calculation of area under curve (AUC) values to evaluate the ability of the different methods to differentiate the two OA groups (39). In addition, relative changes (%) in relaxation times between early OA and advanced OA groups were calculated (100 % * (mean(early OA)/mean(advanced OA))-100). Statistical analyses were performed with SPSS 19.0 (IBM, Armonk, NY, USA) and MATLAB.

Results

Reference methods

Average OARSI grade (±SD) for the early OA group was 1.3±0.3, reflecting the early damage of cartilage (Table 2). For the advanced OA group average grade was 3.2±1.0, indicating more advanced cartilage degeneration (Table 2). In the early and advanced OA groups the OARSI grades varied from 0.9 to 1.5 and from 1.6 to 4.1, respectively. Optical density, a biomarker for PG content was lower in the samples with advanced degeneration compared to early OA specimens (Table 2), although the difference was not statistically significant. Depth-wise profiles showed reduced amounts of PGs throughout the sample depth and a statistically significant difference in the deep cartilage (Figure 1). Similarly, PG content assessed from FTIR measurements of the carbohydrate region was slightly lower in the advanced OA group, although there was no statistical significance (Figure 1, Table 2).

Collagen fibril anisotropy was lower in the advanced OA group, although not significantly (Table 2). Significantly higher anisotropy values were seen in the deep half of the cartilage (Figure 1). Collagen content (amide I absorbance) maps showed higher values in the superficial part of the cartilage as well as in the full-thickness analysis in the early OA group but the difference was not statistically significant (Figure 1, Table 2).

Equilibrium elastic and dynamic modulus were significantly lower in the advanced OA group in comparison to early OA group (Table 2). Water content was increased in the advanced OA group, although not statistically significantly.

MRI

Different MRI techniques responded variably to the cartilage degeneration (Figure 1, Figure 2). A single representative sample from early OA group with an OARSI grade of 0.9 showed a typical tri-laminar appearance in adiabatic $T_{2\rho}$, RAFF, T_2 maps and CW-$T_{1\rho}$ maps with spin-lock frequencies below 1000 Hz (Figure 2), which was also evident in the mean depth-

wise relaxation time profiles (Figure 1). T_1, adiabatic $T_{1\rho}$ and CW-$T_{1\rho}$ at 1 kHz spin-lock had relaxation times decreasing towards the cartilage-bone interface (Figure 1, Figure 2). $T_{1,Gd}$ maps showed a good agreement with the Safranin-O stained microscopy sections and carbohydrate maps, which demonstrated loss of PGs in the superficial cartilage. $T_{1,Gd}$ and DD profiles were similar in shape in both groups (Figure 1). T_{1sat} map was relatively uniform throughout the cartilage depth.

A representative sample with advanced cartilage degeneration (OARSI grade 3.7) showed very high relaxation times in the superficial cartilage for all MRI techniques, except $T_{1,Gd}$, compared to early OA sample (Figure 2). In the advanced OA group, prolongation of the relaxation times was also noted deeper in the cartilage while the typical tri-laminar appearance was not detected in any of the relaxation time maps. In $T_{1,Gd}$ map the superficial zone showed lower relaxation times compared to deep zone. Correspondingly, Safranin-O stained section and carbohydrate map demonstrated fibrillation and loss of PGs in the superficial cartilage. Relaxation time profiles showed a decreasing trend from the surface to deep cartilage for all parameters, except $T_{1,Gd}$, which also had lower relaxation time values (as expected, instead of higher, as was the case for all other parameters) throughout the cartilage depth compared to early OA group (Figure 1).

Zonal analysis revealed significant prolongation of all MRI parameters, except $T_{1,Gd}$, in tangential and full-thickness ROIs for advanced OA specimens compared to early OA group (Table 3). There was no significant difference between the groups in CW-$T_{1\rho}$ (at 1 kHz spin-lock frequency) in full-thickness ROI, although the values showed a trend towards longer relaxation times in the advanced OA group. In the radial zone only DE-T2 and in the transitional ROI, only adiabatic $T_{1\rho}$, adiabatic $T_{2\rho}$, CW-$T_{1\rho}$ (at 500 Hz spin-lock frequency), T_1 and T_{1sat} parameters were significantly longer in the advanced OA group. CW-$T_{1\rho}$ at the lowest spin-lock frequency of 125 Hz showed the characteristics of T_2-data in the early OA group, with transitional zone values higher than those of the tangential zone, also observed in depth-wise profile plots (Figure 1). Compared to T_2 relaxation times, CW-$T_{1\rho}$ values were higher in all ROIs in both groups.

ROC analysis and relative changes

The AUC values from ROC-analysis were high (0.9 to 1.0) in the tangential zone for all parameters except $T_{1,Gd}$ (Table 4), indicating good distinction between early and advanced OA groups. In the transitional zone, AUC values were the highest for adiabatic $T_{1\rho}$, adiabatic $T_{2\rho}$, CW-$T_{1\rho}$ (500 Hz), T_1 and T_{1sat} parameters, in the range of 0.8 to 1 (Table 4). In the radial zone AUC value was high only for DE-T_2. Highest AUC values (0.96 to 1.0) in full-thickness analysis were observed for adiabatic $T_{1\rho}$, adiabatic $T_{2\rho}$, CW-$T_{1\rho}$ (250 and 500 Hz), RAFF and DE-T_2. For tangential zone, the relative changes (%) between the two groups in relaxation times were highest for RAFF, adiabatic $T_{1\rho}$, adiabatic $T_{2\rho}$, CW-$T_{1\rho}$ (125–1000 Hz) and T_{1sat}, with approximately 100 % or more (Table 4). In the transitional zone the relative change for adiabatic $T_{1\rho}$, adiabatic $T_{2\rho}$, CW-$T_{1\rho}$ (all spin-lock powers) and T_{1sat} parameters were in the range of 60 %. Similar relative changes were observed in full-thickness ROI for adiabatic $T_{2\rho}$, CW-$T_{1\rho}$, RAFF, DE-T_2 and T_2 parameters.

Correlation analysis

Correlations between OARSI grade and MRI parameters for pooled data, combining early and advanced OA group, were the highest for adiabatic $T_{1\rho}$, adiabatic $T_{2\rho}$, CW-$T_{1\rho}$ (250 and 500 Hz) and T_{1sat}, in the range of 0.8 (Table 5). Water content correlated only moderately, however still significantly with adiabatic $T_{1\rho}$ and T_{1sat}. Significant correlations were also found between optical density and adiabatic $T_{1\rho}$, adiabatic $T_{2\rho}$, CW-$T_{1\rho}$ (250 and 500) and T_{1sat}. Collagen fibril anisotropy correlated significantly with DE-T_2 and CW-$T_{1\rho}$ (125 Hz). The correlations between equilibrium elastic modulus and MRI parameters were high, approximately 0.8, for adiabatic $T_{1\rho}$, adiabatic $T_{2\rho}$, CW-$T_{1\rho}$ (250 and 500 Hz), RAFF, DE-T_2 and T_{1sat} (Table 5). Furthermore, the equilibrium modulus correlated significantly with OARSI grade and PG content as determined by DD and FTIR (Table 5). Highest correlation coefficients (0.7 to 0.8) between the dynamic modulus and MRI parameters were obtained for adiabatic $T_{1\rho}$, adiabatic $T_{2\rho}$, CW-$T_{1\rho}$ (250 and 500 Hz) and T_{1sat}. In addition, the correlation of dynamic modulus with CW-$T_{1\rho}$ (125 Hz and 1 kHz), RAFF, DE-T_2, T_2 and T_1 was also significant. The dynamic modulus correlated significantly with OARSI grade and water content. The correlation of $T_{1,Gd}$ was not significant with any of the reference parameters. FTIR-derived collagen content, integrated absorbance of amide I region, correlated significantly with the native T_1 relaxation time. There were also significant but weak correlations between carbohydrate region and CW-$T_{1\rho}$ (250 Hz), DE-T_2, T_2 and RAFF.

Discussion

In the present work, quantitative MR imaging was performed to investigate sensitivity of adiabatic $T_{1\rho}$, adiabatic $T_{2\rho}$, CW-$T_{1\rho}$ dispersion (spin-lock frequencies of 125, 250, 500 and 1000 Hz), RAFF, inversion-prepared MT (T_{1sat}), T_2-mapping with adiabatic DE and spin echo techniques, and the dGEMRIC technique (pre- and post-contrast T_1) in detection of degeneration of human articular cartilage. A systematic comparison between different quantitative MRI techniques in human OA is lacking, and previously only few studies have tested and compared several parameters in one OA model (17, 40, 41). All parameters, except $T_{1,Gd,}$ were able to separate early OA cartilage specimens from advanced OA group. In addition, RFR relaxation time parameters and T_{1sat} were highly correlated to OARSI grade and biomechanical parameters.

The pathology of OA in humans has been studied extensively (1, 2). The present study included OA specimens with a wide range of OARSI grades. The early OA group contained relatively intact samples (OARSI grade < 1.5) while the advanced OA group contained samples with more varying degeneration. It is noteworthy that although the samples with low OARSI grade represent almost normal cartilage, completely intact tissue (grade 0) could not be found in these TKA specimens. Conversely, none of the samples included in the study showed total tissue erosion (35). Decrease of the PG content in the superficial cartilage, a typical sign of early OA, was found in the specimens of the early OA group by digital densitometry, although the difference was not statistically significant. More advanced OA samples demonstrated PG loss, surface fibrillation and collagen fibril disorganization which are in agreement with the previous works (1, 36). Furthermore, the biomechanical

measurements were also in accordance with histological findings, showing significantly reduced equilibrium and dynamic elastic moduli in the advanced OA group in comparison to early OA group. Equilibrium elastic modulus is mainly influenced by PGs which contribute to static loading properties of cartilage, while the collagen network is responsible for the dynamic loading properties of cartilage (42). In the present study, the equilibrium elastic modulus also correlated significantly with PG content determined from DD and FTIR measurements.

T_2 relaxation time mapping was performed with spin echo and adiabatic DE contrast preparation techniques, both depicting the classical tri-laminar structure in the early OA group, also previously seen in human and animal cartilage tissue (6, 37, 38). Significant T_2 elevation was noted with both methods in the advanced OA group, which is also consistent with previous studies (6, 8, 43–45). Although T_2 relaxation time is known to be sensitive to the properties of collagen network, the collagen fibril anisotropy and dynamic modulus correlated significantly with only DE-T_2. However, regardless of the differences in statistical significance, the correlation coefficients were nearly the same for both techniques. Also correlations to elastic modulus and OARSI grade were higher for DE-T_2 than for spin echo-based T_2. The different outcomes may be explained by differences in the pulse sequences. The adiabatic pulses in DE-T_2 likely provide more robust inversions with improved refocusing and slightly better resistance to changes due to diffusion processes by the use of two pulses instead of one, thus improving estimation of the T_2 relaxation time.

In previous works, significant correlations between GAG content and dGEMRIC technique have been observed (7, 8, 46, 47). In the present study, the dGEMRIC technique was used to measure the samples after 24-hour immersion in gadolinium contrast agent. Unexpectedly, there were no statistically significant changes in $T_{1,Gd}$ parameter between the sample groups, however, a decreasing trend of $T_{1,Gd}$ values was observed in each ROI in the advanced OA group. Furthermore, the dGEMRIC method did not correlate significantly with any of the reference methods although the depth-wise profiles of $T_{1,Gd}$ and PG content measured by optical density were similar in shape in both OA groups. There were also striking similarities between $T_{1,Gd}$ and the carbohydrate maps and Safranin-O stained sections. However, there was a statistically significant difference in PG content between the groups only in deep cartilage, as determined by DD, which might explain these surprising findings. Also, in a previous *in vitro* study the dGEMRIC technique could not distinguish between early hip OA and reference cartilage (48). The pre-contrast native T_1-mapping has been previously linked to the water content of cartilage (9), however, no significant correlations with water content were found in the present study. Instead, T_1 showed significant elevation in the advanced OA group and significant correlations to both equilibrium and dynamic moduli and OARSI grade.

Both CW-$T_{1\rho}$ and adiabatic $T_{1\rho}$ were sensitive to cartilage degeneration in the present study. CW-$T_{1\rho}$ has been found sensitive to cartilage degeneration in many earlier studies and has been primarily linked to PG content (15). In recent studies adiabatic $T_{1\rho}$ was found to be sensitive to degradation in trypsin-digested bovine cartilage (17) and to early OA changes in a rabbit model of anterior cruciate ligament transection (23). In the present work, adiabatic $T_{1\rho}$ correlated strongly with biomechanical measurements and OARSI grade and moderately

with water content and optical density. In previous clinical studies, CW-$T_{1\rho}$ mapping at spin-lock frequency of 500 Hz was able to separate healthy and OA patients at 3T (49) as well as post-traumatic cartilage degeneration after anterior cruciate ligament reconstruction (50). CW-$T_{1\rho}$ (spin-lock = 500 Hz) has been also reported to correlate to arthroscopically confirmed cartilage degeneration at 1.5 T (51). In the current work, CW-$T_{1\rho}$ correlated significantly to biomechanical parameters, water content, optical density and OARSI grade, with highest correlations at spin-lock frequencies of 250 and 500 Hz. The use of CW-$T_{1\rho}$ in human studies has been limited to low spin lock fields due to specific absorption rate (SAR) limitations.

The CW-$T_{1\rho}$ data showed significant dispersion in the current study, which has also been previously reported in human cartilage (21). The tri-laminar appearance diminished in CW-$T_{1\rho}$ relaxation time maps with increasing spin-lock frequency owing to reduced contribution from dipolar interactions (52). Most evidently laminar appearance was similar to T_2-maps at spin-lock frequency of 125 Hz, as the $T_{1\rho}$ experiment approaches T_2 experiment when the spin-locking frequency approaches zero (15). PG content as measured with optical density correlated significantly with CW-$T_{1\rho}$ at spin-lock frequencies of 250 and 500 Hz but not at 125 Hz. Surprisingly, at spin-lock frequency of 1000 Hz, the correlation to PG content as determined by optical density was also not significant. At 125 Hz spin-lock frequency, CW-$T_{1\rho}$ correlated significantly with collagen anisotropy, which is in agreement with the theoretical expectation.

Previously, adiabatic $T_{2\rho}$ was reported sensitive to early cartilage degeneration in an animal model of OA (23). In the present study with human tissue, $T_{2\rho}$ was significantly elevated in the advanced OA group in the superficial and transitional zone as well as in the full-thickness ROI. $T_{2\rho}$ also correlated strongly with biomechanical properties and OARSI grade indicating high sensitivity to cartilage degeneration. Furthermore, another RFR parameter, RAFF, has previously been shown to be sensitive to cartilage degeneration by trypsin induced PG depletion (17). In the present study RAFF was also able to separate the two OA groups and correlated significantly with biomechanical parameters and OARSI grade. Operating in low power regime, RAFF provides reduction to SAR and has already been implemented for imaging of human brain at 4 T (18, 53). Further improvements to SAR issues could be obtained using RAFF operating in higher rank rotating frames (54).

In conventional MT experiments irradiation pulse length is limited due to RF energy deposition limits, thus potentially causing instability to the estimation of MT parameters. Inversion-prepared MT differs from conventional MT experiment by applying an inversion pulse prior to off-resonance saturation pulse, thus improving the dynamic range of the measurement, providing more robust estimation of MT parameters and also alleviating SAR problems of MT experiments as shorter saturation pulses can be applied (27). The MT effect in cartilage has been generally linked to the collagen content and interaction of water with collagen/collagen-bound water (10), although reports on PG association also exist (55, 56). T_{1sat} showed significant differences between the OA groups in the present work and was highly correlated with biomechanical parameters and OARSI grade, showing also moderate correlations with water content and optical density. In a previous study, T_{1sat} was able to differentiate trypsin- and non-digested bovine cartilage (17). In an animal model of early

OA, no significant differences between injured and contralateral knees were reported for T_{1sat}, however, the cartilage degeneration was much milder than in the trypsin-digestion study (23).

The ROC analysis was performed to investigate diagnostic accuracy of the MRI parameters to separate early and advanced OA specimens. In previous clinical studies, the AUC of CW-$T_{1\rho}$ was better compared to T_2 (39, 57). Furthermore, CW-$T_{1\rho}$ has been reported as more sensitive biomarker for cartilage degeneration than T_2 (39, 49, 58, 59). In the present study, all MRI parameters except $T_{1,Gd}$ had excellent AUC values (0.9–1.0) in the tangential and full-thickness ROI. In the transitional zone, ROC analysis revealed differences between MRI parameters and AUC values were still good, over 0.8, for adiabatic $T_{1\rho}$, adiabatic $T_{2\rho}$, CW-$T_{1\rho}$ (1 kHz), DE-T_2, T_1 and T_{1sat}. This further emphasizes the importance of the zonal evaluation of quantitative MRI parameters in articular cartilage. RFR relaxation parameters also correlated well with OARSI grade in the present work. Previously, there was no significant correlation with $T_{1\rho}$ or T_2 and histological Mankin score in a study with osteoarthritic human specimens (60). This discrepancy can be possibly explained by the different histological scoring methods used as the OARSI grading system has a larger dynamic range for early stages of OA in comparison with Mankin grading (32). Highest relative changes for MRI relaxation parameters were obtained for CW-$T_{1\rho}$, adiabatic $T_{2\rho}$, RAFF, DE-T_2, T_2 in the full-thickness ROI. For adiabatic $T_{1\rho}$, RAFF and T_{1sat} the relative changes are in accordance with values reported in PG-depleted bovine cartilage (17). In a previous study with human OA cartilage at 4 T, the relative elevation of CW-$T_{1\rho}$ (500 Hz) was reported higher than that of T_2 (58), which were in this work approximately the same in full-thickness ROI. The present results indicate a high sensitivity of RFR methods for changes in slow macromolecular motion which occur in cartilage during degeneration (11, 15). In particular, the adiabatic RFR methods using frequency swept pulses offer robustness to B_0 and B_1 field inhomogeneities (13), overcoming limitations posed by CW-$T_{1\rho}$ implementations, which are clinically relevant. In addition, inversion-prepared MT experiment and DE-T_2 performed well in the present study, however, the disadvantage of T_2 for cartilage imaging is its orientation dependence in relation to B_0 field (5).

This study was limited by the relatively small number of samples, which may have affected the power of statistical comparisons. MRI was performed at field strength of 9.4 T, which is significantly higher than in most clinical scanners. Also, the measurement conditions for *ex vivo* specimens differ from their real physiological environment. Consequently, *in vivo* studies, possibly at lower field strengths, should be performed to confirm the findings of the present study. Quantitative MRI parameters were not evaluated in completely healthy human cartilage specimens in our study, due to its unavailability. The zonal evaluation of the advanced OA samples may have been hindered by tissue erosion which may affect the comparison of the ROIs of the cartilage layers between early and advanced OA. Furthermore, the very high relaxation times observed in the superficial cartilage in advanced OA samples was most likely caused by a small amount of residual PBS solution left on the surfaces of the samples prior to imaging (61). However, the thicknesses of the full-thickness ROIs were compared against the thicknesses derived from microscopy images. In clinical studies, the presented measurement of a wide range of quantitative MRI parameters is not possible due to time constraints and thus the most sensitive parameters should be selected.

In conclusion, a comprehensive comparison of different qMRI techniques revealed that inversion prepared MT, and rotating frame MRI relaxation parameters, which are sensitive to slow macromolecular motion, efficiently detected degeneration of human articular cartilage *ex vivo* and are highly correlated to the histological grade and biomechanical parameters of the tissue. In the future, clinical studies with RFR techniques employing adiabatic RF pulses may be preferable due to increased flexibility for dealing with SAR constraints and reduced B_0 and B_1 inhomogeneity issues.

Acknowledgements

This study was supported by the Academy of Finland (grants 128603, 260321), NIH grant P41 EB015894, Foundation for Advanced Technology of Eastern Finland, and National Doctoral Programme of Musculoskeletal Disorders and Biomaterials in Finland.

References

1. Buckwalter JA, Mankin HJ. Articular cartilage: Degeneration and osteoarthritis, repair, regeneration, and transplantation. Instr Course Lect. 1998; 47:487–504. [PubMed: 9571450]
2. Goldring MB, Goldring SR. Articular cartilage and subchondral bone in the pathogenesis of osteoarthritis. Ann N Y Acad Sci. 2010; 1192:230–237. [PubMed: 20392241]
3. Li X, Majumdar S. Quantitative MRI of articular cartilage and its clinical applications. J Magn Reson Imaging. 2013; 38(5):991–1008. [PubMed: 24115571]
4. Nieminen MT, Nissi MJ, Mattila L, Kiviranta I. Evaluation of chondral repair using quantitative MRI. J Magn Reson Imaging. 2012; 36(6):1287–1299. [PubMed: 23165732]
5. Xia Y. Relaxation anisotropy in cartilage by NMR microscopy (muMRI) at 14-microm resolution. Magn Reson Med. 1998; 39(6):941–949. [PubMed: 9621918]
6. Nieminen MT, Toyras J, Rieppo J, Hakumaki JM, Silvennoinen J, Helminen HJ, Jurvelin JS. Quantitative MR microscopy of enzymatically degraded articular cartilage. Magn Reson Med. 2000; 43(5):676–681. [PubMed: 10800032]
7. Bashir A, Gray ML, Burstein D. Gd-DTPA2- as a measure of cartilage degradation. Magn Reson Med. 1996; 36(5):665–673. [PubMed: 8916016]
8. Nissi MJ, Toyras J, Laasanen MS, Rieppo J, Saarakkala S, Lappalainen R, Jurvelin JS, Nieminen MT. Proteoglycan and collagen sensitive MRI evaluation of normal and degenerated articular cartilage. J Orthop Res. 2004; 22(3):557–564. [PubMed: 15099635]
9. Berberat JE, Nissi MJ, Jurvelin JS, Nieminen MT. Assessment of interstitial water content of articular cartilage with T1 relaxation. Magn Reson Imaging. 2009; 27(5):727–732. [PubMed: 19056195]
10. Gray ML, Burstein D, Lesperance LM, Gehrke L. Magnetization transfer in cartilage and its constituent macromolecules. Magn Reson Med. 1995; 34(3):319–325. [PubMed: 7500869]
11. Mangia S, Liimatainen T, Garwood M, Michaeli S. Rotating frame relaxation during adiabatic pulses vs. conventional spin lock: Simulations and experimental results at 4 T. Magn Reson Imaging. 2009; 27(8):1074–1087. [PubMed: 19559559]
12. Jokivarsi KT, Niskanen JP, Michaeli S, Grohn HI, Garwood M, Kauppinen RA, Grohn OH. Quantitative assessment of water pools by T 1 rho and T 2 rho MRI in acute cerebral ischemia of the rat. J Cereb Blood Flow Metab. 2009; 29(1):206–216. [PubMed: 18827834]
13. Garwood M, DelaBarre L. The return of the frequency sweep: Designing adiabatic pulses for contemporary NMR. J Magn Reson. 2001; 153(2):155–177. [PubMed: 11740891]
14. Duvvuri U, Goldberg AD, Kranz JK, Hoang L, Reddy R, Wehrli FW, Wand AJ, Englander SW, Leigh JS. Water magnetic relaxation dispersion in biological systems: The contribution of proton exchange and implications for the noninvasive detection of cartilage degradation. Proc Natl Acad Sci U S A. 2001; 98(22):12479–12484. [PubMed: 11606754]

15. Borthakur A, Mellon E, Niyogi S, Witschey W, Kneeland JB, Reddy R. Sodium and T1rho MRI for molecular and diagnostic imaging of articular cartilage. NMR Biomed. 2006; 19(7):781–821. [PubMed: 17075961]
16. Mangia S, Traaseth NJ, Veglia G, Garwood M, Michaeli S. Probing slow protein dynamics by adiabatic R(1rho) and R(2rho) NMR experiments. J Am Chem Soc. 2010; 132(29):9979–9981. [PubMed: 20590094]
17. Ellermann J, Ling W, Nissi MJ, Arendt E, Carlson CS, Garwood M, Michaeli S, Mangia S. MRI rotating frame relaxation measurements for articular cartilage assessment. Magn Reson Imaging. 2013; 31(9):1537–1543. [PubMed: 23993794]
18. Liimatainen T, Sorce DJ, O'Connell R, Garwood M, Michaeli S. MRI contrast from relaxation along a fictitious field (RAFF). Magn Reson Med. 2010; 64(4):983–994. [PubMed: 20740665]
19. Duvvuri U, Reddy R, Patel SD, Kaufman JH, Kneeland JB, Leigh JS. T1rho-relaxation in articular cartilage: Effects of enzymatic degradation. Magn Reson Med. 1997; 38(6):863–867. [PubMed: 9402184]
20. Duvvuri U, Kudchodkar S, Reddy R, Leigh JS. T(1rho) relaxation can assess longitudinal proteoglycan loss from articular cartilage in vitro. Osteoarthritis Cartilage. 2002; 10(11):838–844. [PubMed: 12435327]
21. Regatte RR, Akella SV, Wheaton AJ, Borthakur A, Kneeland JB, Reddy R. T 1 rho-relaxation mapping of human femoral-tibial cartilage in vivo. J Magn Reson Imaging. 2003; 18(3):336–341. [PubMed: 12938129]
22. Keenan KE, Besier TF, Pauly JM, Han E, Rosenberg J, Smith RL, Delp SL, Beaupre GS, Gold GE. Prediction of glycosaminoglycan content in human cartilage by age, T1rho and T2 MRI. Osteoarthritis Cartilage. 2011; 19(2):171–179. [PubMed: 21112409]
23. Rautiainen J, Nissi MJ, Liimatainen T, Herzog W, Korhonen RK, Nieminen MT. Adiabatic rotating frame relaxation of MRI reveals early cartilage degeneration in a rabbit model of anterior cruciate ligament transection. Osteoarthritis Cartilage. 2014 accepted for publication.
24. Rautiainen, J., Salo, E., Tiitu, V., Finnilä, MAJ., Aho, O., Saarakkala, S., Lehenkari, P., Ellermann, J., Nissi, MJ., Nieminen, MT. Proc. Intl. Soc. Magn. Reson. Med. Italy: Milan; 2014. Assessment of Human Articular Cartilage Using Novel Quantitative MRI Relaxation Parameters with Correlation to Histology and Biomechanical Properties; p. 300
25. Michaeli S, Sorce DJ, Springer CS Jr, Ugurbil K, Garwood M. T1rho MRI contrast in the human brain: Modulation of the longitudinal rotating frame relaxation shutter-speed during an adiabatic RF pulse. J Magn Reson. 2006; 181(1):135–147. [PubMed: 16675277]
26. Michaeli S, Sorce DJ, Idiyatullin D, Ugurbil K, Garwood M. Transverse relaxation in the rotating frame induced by chemical exchange. J Magn Reson. 2004; 169(2):293–299. [PubMed: 15261625]
27. Mangia S, De Martino F, Liimatainen T, Garwood M, Michaeli S. Magnetization transfer using inversion recovery during off-resonance irradiation. Magn Reson Imaging. 2011; 29(10):1346–1350. [PubMed: 21601405]
28. Grohn HI, Michaeli S, Garwood M, Kauppinen RA, Grohn OH. Quantitative T(1rho) and adiabatic carr-purcell T2 magnetic resonance imaging of human occipital lobe at 4 T. Magn Reson Med. 2005; 54(1):14–19. [PubMed: 15968651]
29. Korhonen RK, Laasanen MS, Toyras J, Rieppo J, Hirvonen J, Helminen HJ, Jurvelin JS. Comparison of the equilibrium response of articular cartilage in unconfined compression, confined compression and indentation. J Biomech. 2002; 35(7):903–909. [PubMed: 12052392]
30. Toyras J, Laasanen MS, Saarakkala S, Lammi MJ, Rieppo J, Kurkijarvi J, Lappalainen R, Jurvelin JS. Speed of sound in normal and degenerated bovine articular cartilage. Ultrasound Med Biol. 2003; 29(3):447–454. [PubMed: 12706196]
31. Kiraly K, Lammi M, Arokoski J, Lapvetelainen T, Tammi M, Helminen H, Kiviranta I. Safranin O reduces loss of glycosaminoglycans from bovine articular cartilage during histological specimen preparation. Histochem J. 1996; 28(2):99–107. [PubMed: 8737291]
32. Pritzker KP, Gay S, Jimenez SA, Ostergaard K, Pelletier JP, Revell PA, Salter D, van den Berg WB. Osteoarthritis cartilage histopathology: Grading and staging. Osteoarthritis Cartilage. 2006; 14(1): 13–29. [PubMed: 16242352]

33. Rieppo J, Hallikainen J, Jurvelin JS, Kiviranta I, Helminen HJ, Hyttinen MM. Practical considerations in the use of polarized light microscopy in the analysis of the collagen network in articular cartilage. Microsc Res Tech. 2008; 71(4):279–287. [PubMed: 18072283]
34. Camacho NP, West P, Torzilli PA, Mendelsohn R. FTIR microscopic imaging of collagen and proteoglycan in bovine cartilage. Biopolymers. 2001; 62(1):1–8. [PubMed: 11135186]
35. Rieppo L, Saarakkala S, Narhi T, Helminen HJ, Jurvelin JS, Rieppo J. Application of second derivative spectroscopy for increasing molecular specificity of fourier transform infrared spectroscopic imaging of articular cartilage. Osteoarthritis Cartilage. 2012; 20(5):451–459. [PubMed: 22321720]
36. Saarakkala S, Julkunen P, Kiviranta P, Makitalo J, Jurvelin JS, Korhonen RK. Depth-wise progression of osteoarthritis in human articular cartilage: Investigation of composition, structure and biomechanics. Osteoarthritis Cartilage. 2010; 18(1):73–81. [PubMed: 19733642]
37. Xia Y, Moody JB, Burton-Wurster N, Lust G. Quantitative in situ correlation between microscopic MRI and polarized light microscopy studies of articular cartilage. Osteoarthritis Cartilage. 2001; 9(5):393–406. [PubMed: 11467887]
38. Nissi MJ, Rieppo J, Toyras J, Laasanen MS, Kiviranta I, Jurvelin JS, Nieminen MT. T(2) relaxation time mapping reveals age- and species-related diversity of collagen network architecture in articular cartilage. Osteoarthritis Cartilage. 2006; 14(12):1265–1271. [PubMed: 16843689]
39. Takayama Y, Hatakenaka M, Tsushima H, Okazaki K, Yoshiura T, Yonezawa M, Nishikawa K, Iwamoto Y, Honda H. T1rho is superior to T2 mapping for the evaluation of articular cartilage denaturalization with osteoarthritis: Radiological-pathological correlation after total knee arthroplasty. Eur J Radiol. 2013; 82(4):e192–e198. [PubMed: 23265927]
40. Stanisz GJ, Odrobina EE, Pun J, Escaravage M, Graham SJ, Bronskill MJ, Henkelman RM. T1, T2 relaxation and magnetization transfer in tissue at 3T. Magn Reson Med. 2005; 54(3):507–512. [PubMed: 16086319]
41. Lin PC, Reiter DA, Spencer RG. Classification of degraded cartilage through multiparametric MRI analysis. J Magn Reson. 2009; 201(1):61–71. [PubMed: 19762258]
42. Korhonen RK, Laasanen MS, Toyras J, Lappalainen R, Helminen HJ, Jurvelin JS. Fibril reinforced poroelastic model predicts specifically mechanical behavior of normal, proteoglycan depleted and collagen degraded articular cartilage. J Biomech. 2003; 36(9):1373–1379. [PubMed: 12893046]
43. Mosher TJ, Dardzinski BJ, Smith MB. Human articular cartilage: Influence of aging and early symptomatic degeneration on the spatial variation of T2--preliminary findings at 3 T. Radiology. 2000; 214(1):259–266. [PubMed: 10644134]
44. Lammentausta E, Kiviranta P, Toyras J, Hyttinen MM, Kiviranta I, Nieminen MT, Jurvelin JS. Quantitative MRI of parallel changes of articular cartilage and underlying trabecular bone in degeneration. Osteoarthritis Cartilage. 2007; 15(10):1149–1157. [PubMed: 17502160]
45. Kijowski R, Blankenbaker DG, Munoz Del Rio A, Baer GS, Graf BK. Evaluation of the articular cartilage of the knee joint: Value of adding a T2 mapping sequence to a routine MR imaging protocol. Radiology. 2013; 267(2):503–513. [PubMed: 23297335]
46. Nieminen MT, Rieppo J, Silvennoinen J, Toyras J, Hakumaki JM, Hyttinen MM, Helminen HJ, Jurvelin JS. Spatial assessment of articular cartilage proteoglycans with gd-DTPA-enhanced T1 imaging. Magn Reson Med. 2002; 48(4):640–648. [PubMed: 12353281]
47. Tiderius CJ, Olsson LE, Leander P, Ekberg O, Dahlberg L. Delayed gadolinium-enhanced MRI of cartilage (dGEMRIC) in early knee osteoarthritis. Magn Reson Med. 2003; 49(3):488–492. [PubMed: 12594751]
48. Stubendorff JJ, Lammentausta E, Struglics A, Lindberg L, Heinegard D, Dahlberg LE. Is cartilage sGAG content related to early changes in cartilage disease? implications for interpretation of dGEMRIC. Osteoarthritis Cartilage. 2012; 20(5):396–404. [PubMed: 22334095]
49. Li X, Benjamin Ma C, Link TM, Castillo DD, Blumenkrantz G, Lozano J, Carballido-Gamio J, Ries M, Majumdar S. In vivo T(1rho) and T(2) mapping of articular cartilage in osteoarthritis of the knee using 3 T MRI. Osteoarthritis Cartilage. 2007; 15(7):789–797. [PubMed: 17307365]
50. Su F, Hilton JF, Nardo L, Wu S, Liang F, Link TM, Ma CB, Li X. Cartilage morphology and T1rho and T2 quantification in ACL-reconstructed knees: A 2-year follow-up. Osteoarthritis Cartilage. 2013; 21(8):1058–1067. [PubMed: 23707754]

51. Witschey WR, Borthakur A, Fenty M, Kneeland BJ, Lonner JH, McArdle EL, Sochor M, Reddy R. T1rho MRI quantification of arthroscopically confirmed cartilage degeneration. Magn Reson Med. 2010; 63(5):1376–1382. [PubMed: 20432308]
52. Akella SV, Regatte RR, Wheaton AJ, Borthakur A, Reddy R. Reduction of residual dipolar interaction in cartilage by spin-lock technique. Magn Reson Med. 2004; 52(5):1103–1109. [PubMed: 15508163]
53. Liimatainen T, Mangia S, Ling W, Ellermann J, Sorce DJ, Garwood M, Michaeli S. Relaxation dispersion in MRI induced by fictitious magnetic fields. J Magn Reson. 2011; 209(2):269–276. [PubMed: 21334231]
54. Liimatainen T, Hakkarainen H, Mangia S, Huttunen JM, Storino C, Idiyatullin D, Sorce D, Garwood M, Michaeli S. MRI contrasts in high rank rotating frames. Magn Reson Med. 2014 Epub ahead of print.
55. Lattanzio PJ, Marshall KW, Damyanovich AZ, Peemoeller H. Macromolecule and water magnetization exchange modeling in articular cartilage. Magn Reson Med. 2000; 44(6):840–851. [PubMed: 11108620]
56. Stikov N, Keenan KE, Pauly JM, Smith RL, Dougherty RF, Gold GE. Cross-relaxation imaging of human articular cartilage. Magn Reson Med. 2011; 66(3):725–734. [PubMed: 21416504]
57. Nishioka H, Hirose J, Nakamura E, Okamoto N, Karasugi T, Taniwaki T, Okada T, Yamashita Y, Mizuta H. Detecting ICRS grade 1 cartilage lesions in anterior cruciate ligament injury using T1rho and T2 mapping. Eur J Radiol. 2013; 82(9):1499–1505. [PubMed: 23743050]
58. Regatte RR, Akella SV, Lonner JH, Kneeland JB, Reddy R. T1rho relaxation mapping in human osteoarthritis (OA) cartilage: Comparison of T1rho with T2. J Magn Reson Imaging. 2006; 23(4): 547–553. [PubMed: 16523468]
59. Stahl R, Luke A, Li X, Carballido-Gamio J, Ma CB, Majumdar S, Link TM. T1rho, T2 and focal knee cartilage abnormalities in physically active and sedentary healthy subjects versus early OA patients--a 3.0-tesla MRI study. Eur Radiol. 2009; 19(1):132–143. [PubMed: 18709373]
60. Li X, Cheng J, Lin K, Saadat E, Bolbos RI, Jobke B, Ries MD, Horvai A, Link TM, Majumdar S. Quantitative MRI using T1rho and T2 in human osteoarthritic cartilage specimens: Correlation with biochemical measurements and histology. Magn Reson Imaging. 2011; 29(3):324–334. [PubMed: 21130590]
61. Rautiainen J, Lehto LJ, Tiitu V, Kiekara O, Pulkkinen H, Brunott A, van Weeren R, Brommer H, Brama PA, Ellermann J, Kiviranta I, Nieminen MT, Nissi MJ. Osteochondral repair: Evaluation with sweep imaging with fourier transform in an equine model. Radiology. 2013; 269(1):113–121. [PubMed: 23674789]

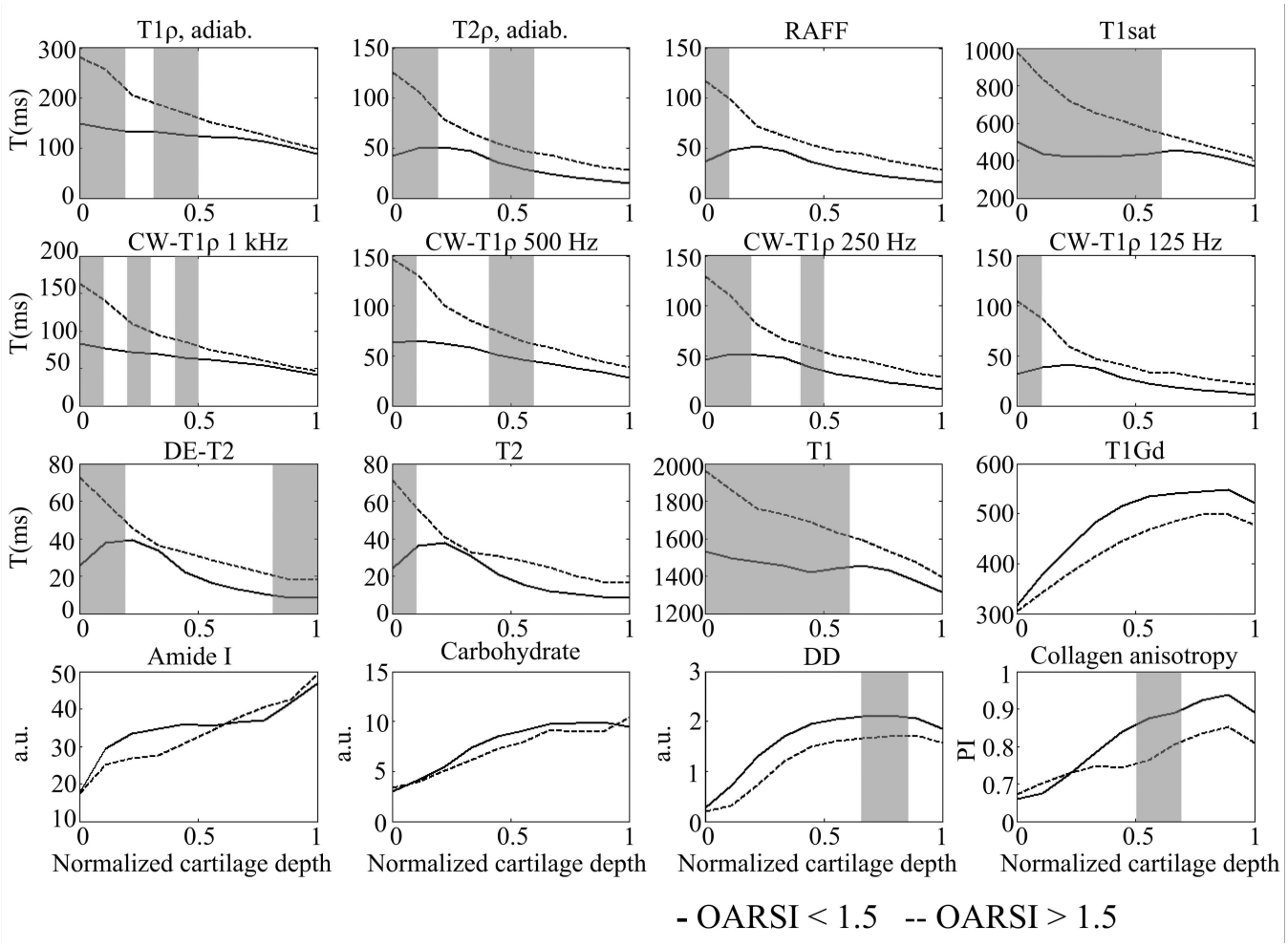

Figure 1.

Mean depth-wise profiles of MRI relaxation time parameters (adiabatic $T_{1\rho}$, adiabatic $T_{2\rho}$, RAFF, T_{1sat}, CW-$T_{1\rho}$ (spin-lock frequencies 1000, 500, 250 and 125 Hz), DE-T_2, T_2, T_1, $T_{1,Gd}$) and reference methods (FTIR-derived absorbance of amide I and carbohydrate regions, optical density (measure of PG content) and collagen anisotropy (parallelism index)) in early (OARSI < 1.5) and advanced OA (OARSI > 1.5) group. Grey background indicates statistically significant difference between the groups ($P < 0.05$, Mann-Whitney U-test).

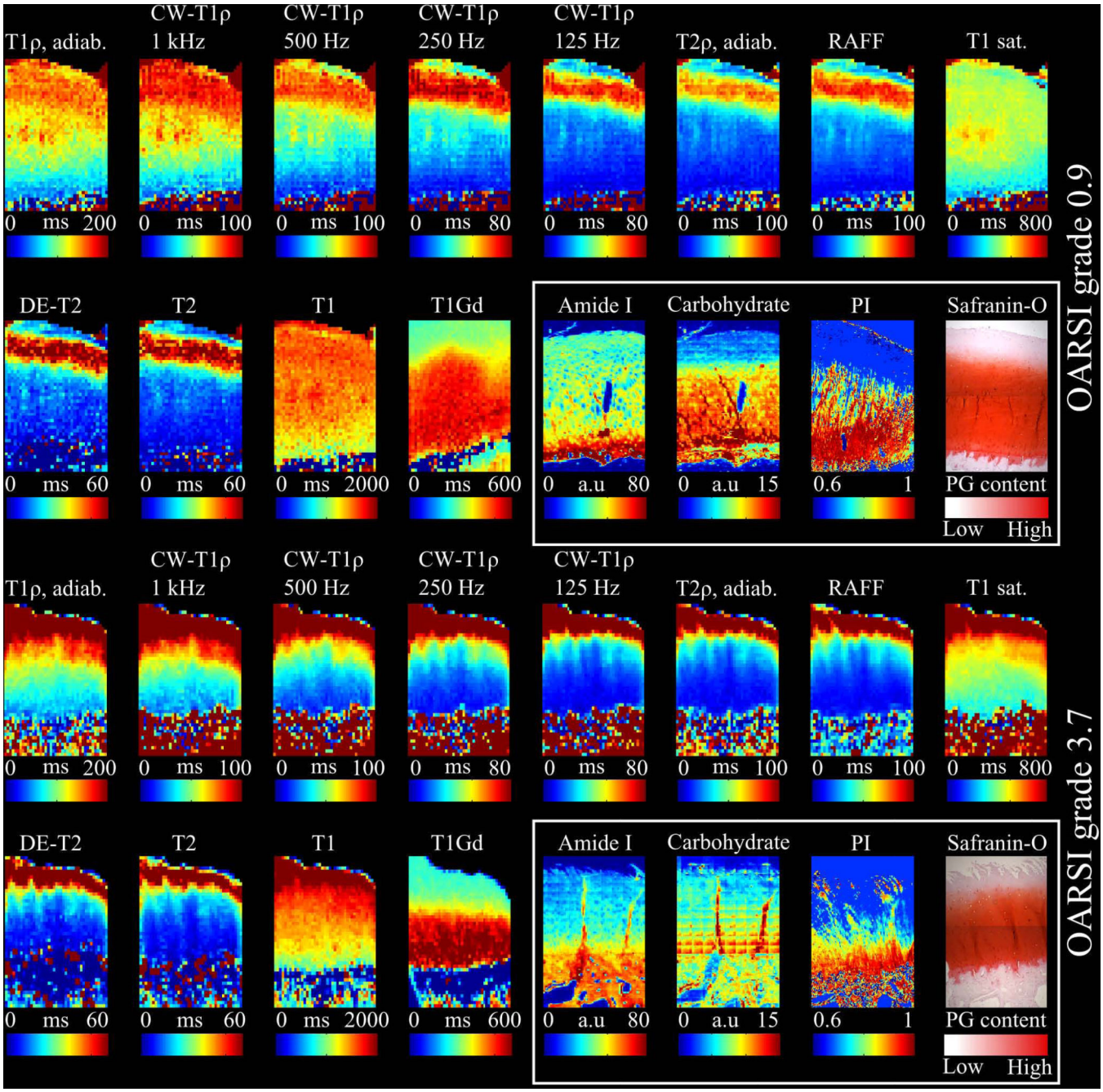

Figure 2.

Representative MRI relaxation time maps (adiabatic $T_{1\rho}$, CW-$T_{1\rho}$ (spin-lock frequencies 1000, 500, 250 and 125 Hz) adiabatic $T_{2\rho}$, RAFF, T_{1sat}, DE-T_2, T_2, T_1, $T_{1,Gd}$), of early and advanced OA sample. Safranin-O stained microscopy section, collagen anisotropy map, amide I and carbohydrate region absorbance maps (white box) are shown for reference revealing superficial PG depletion in the early OA sample. CW-$T_{1\rho}$ dispersion is shown with different spin-locking frequencies while T_2-maps demonstrate tri-laminar structure of

cartilage. Advanced OA sample shows superficial tissue erosion, PG loss and collagen disorganization which is seen as elevated relaxation times in MRI relaxation time maps.

Table 1

Measurement parameters for the magnetization preparation block for different contrasts and the readout sequence.

Contrast	Preparation parameters	Pulse power
Adiabatic $T_{1\rho}$	*Train of 0, 4, 8, 12 and 24 HS1 AFP pulses, pulse duration 4.5 ms	$\gamma B_{1,max}$ = 2.5 kHz
Adiabatic $T_{2\rho}$	AFP pulse train* between HS1 AHP pulses, pulse duration 4.5 ms	$\gamma B_{1,max}$ = 2.5 kHz
CW $T_{1\rho}$ dispersion	CW spin-lock pulses of 0, 10, 20, 40, 80 and 160 ms between HS1 AHP and HS1 AHP-back pulses	γB_1 = 125, 250, 500, 1000 Hz
RAFF	Train of 0, 2, 4 and 6 RAFF pulses, pulse duration 9 ms	$\gamma B_{1,max}$ = 625 Hz
Adiabatic DE-T_2	two HS1 AFP pulses, TE = 4, 8, 16, 32, 64, 128 ms, TR = 5 s	-
T_2	TE = 4, 8, 16, 32, 64, 128 ms, TR = 5 s	-
T_1 & $T_{1,Gd}$	TE = 10 m, TR = 80, 160, 320, 640, 1280, 2560, 5120 ms	-
T_1 saturation	0.1, 0.2, 0.4, 0.8, 1.6, 3.5 and 7.0 s off-resonance CW irradiation at 10 kHz offset with inversion preparation	γB_1 = 250 Hz
FSE readout	TR = 5 s, ETL = 4, TE_{eff} = 5 ms, 256x128 matrix size, slice thickness 1 mm, FOV 16×16 mm	-

AFP = adiabatic full-passage, AHP = adiabatic half-passage, CW = continuous wave, DE = double echo, FSE = fast spin echo, RAFF = relaxation along a fictitious field, TE = time-to-echo, TR = time-to-repetition.

Table 2

Absolute values (mean ± 1 SD) for full cartilage thickness of equilibrium and dynamic moduli, water content, optical density, collagen fibril anisotropy (parallelism index, PI), collagen content from FTIR (amide I absorbance), proteoglycan content from FTIR (carbohydrate absorbance) and OARSI grade.

	Early OA	Advanced OA	*P*-value
Equilibrium modulus (MPa)	1.2 ± 0.3	0.2 ± 0.3	**0.003**
Dynamic modulus (MPa)	6.8 ± 1.7	1.9 ± 2.3	**0.006**
Water content (%)	74.3 ± 2.5	77.2 ± 4.6	0.32
Optical density (a.u.)	1.7 ± 0.3	1.3 ± 0.4	0.06
PI, collagen anisotropy	0.83 ± 0.05	0.77 ± 0.06	0.07
Amide I (a.u.)	36.5 ± 5.5	32.7 ± 5.6	0.16
Carbohydrate (a.u.)	8.0 ± 1.6	7.0 ± 1.1	0.21
OARSI grade	1.3 ± 0.3	3.2 ± 1.0	**0.003**

$P < 0.05$ in boldface

Table 3

Relaxation time values (±1 SD) of adiabatic $T_{1\rho}$, adiabatic $T_{2\rho}$, continuous wave $T_{1\rho}$, RAFF, double echo (DE) T_2, spin echo T_2, T_1, $T_{1(Gd)}$ and T_{1sat} parameters in early ($n = 5$) and advanced OA ($n = 9$) groups.

OARSI < 1.5 (*n* = 5) ROI (mean ± 1SD)				
Parameter	**Tangential (ms)**	**Transitional (ms)**	**Radial (ms)**	**Full (ms)**
$T_{1\rho,Adiab.}$	149.7 ± 16.8	131.7 ± 13.7	102.6 ± 11.0	116.1 ± 10.5
$T_{2\rho,Adiab.}$	46.9 ± 12.7	47.8 ± 10.9	23.2 ± 5.5	32.7 ± 4.2
CW-$T_{1\rho}$ (1 kHz)	84.7 ± 13.8	69.6 ± 8.3	53.2 ± 7.2	61.2 ± 5.5
CW-$T_{1\rho}$ (500 Hz)	67.2 ± 11.2	59.0 ± 9.1	35.5 ± 3.0	45.8 ± 4.1
CW-$T_{1\rho}$ (250 Hz)	50.9 ± 10.0	48.1 ± 12.3	26.2 ± 6.7	35.0 ± 6.1
CW-$T_{1\rho}$ (125 Hz)	34.9 ± 7.3	38.1 ± 15.0	16.7 ± 4.0	25.0 ± 7.0
RAFF	39.9 ± 2.2	48.4 ± 18.1	20.7 ± 4.6	31.1 ± 8.3
DE-T_2	29.6 ± 9.7	36.2 ± 10.9	11.4 ± 2.4	20.9 ± 3.9
T_2	26.4 ± 6.7	34.8 ± 11.1	11.4 ± 1.8	20.0 ± 4.0
T_1	1558.9 ± 43.9	1458.7 ± 80.3	1320.5 ± 120.3	1390.4 ± 86.9
$T_{1,Gd}$	324.5 ± 43.8	429.0 ± 86.0	527.5 ± 41.5	482.1 ± 53.2
$T_{1sat.}$	506.3 ± 77.4	424.0 ± 30.4	453.3 ± 71.1	444.7 ± 37.9
OARSI > 1.5 ($n = 9$)				
$T_{1\rho,Adiab.}$	**287.0 ± 68.7****	**206.7 ± 60.0***	111.8 ± 23.2	**153.0 ± 23.8****
$T_{2\rho,Adiab.}$	**123.9 ± 37.7****	**80.6 ± 27.5***	32.4 ± 11.4	**53.2 ± 11.6****
CW-$T_{1\rho}$ (1 kHz)	**164.1 ± 43.5****	111.0 ± 41.7	55.5 ± 14.9	80.2 ± 21.3
CW-$T_{1\rho}$ (500 Hz)	**140.9 ± 50.3****	**96.8 ± 38.5***	44.1 ± 14.5	**69.3 ± 15.0****
CW-$T_{1\rho}$ (250 Hz)	**118.2 ± 41.7****	79.7 ± 33.2	32.6 ± 12.7	**54.7 ± 12.1****
CW-$T_{1\rho}$ (125 Hz)	**90.6 ± 48.5***	58.3 ± 33.5	23.2 ± 10.0	**40.2 ± 13.2***
RAFF	**109.1 ± 43.7***	74.8 ± 32.5	33.3 ± 11.8	**50.6 ± 11.8****
DE-T_2	**79.7 ± 23.7****	55.1 ± 19.6	**21.4 ± 8.4***	**34.8 ± 8.3****
T_2	**70.6 ± 22.8****	50.1 ± 17.3	20.3 ± 8.8	**32.0 ± 8.8***
T_1	**1966.10 ± 262.6***	**1781.2 ± 228.8****	1428.3 ± 127.9	**1565.7 ± 21.0***
$T_{1,Gd}$	318.2 ± 54.2	376.1 ± 88.6	472.3 ± 106.4	434.6 ± 98.5
T_{1sat}	**980.2 ± 201.0****	**710.5 ± 193.7****	470.4 ± 100.0	**582.8 ± 96.4***

*$P < 0.05$

**$P < 0.01$ in boldface

Table 4

Relative difference (100%*(mean(early OA)/mean(advanced OA))-100) in the average relaxation time values and area under curve values (AUC) between mild and advanced OA groups.

Parameter	Tangential	Transitional	Radial	Full
$T_{1\rho,Adiab.}$	**91.7 %, AUC = 1.00**	**57.0 %, AUC = 0.87**	8.9 %, AUC = 0.64	**31.7 %, AUC = 0.98**
$T_{2\rho,Adiab.}$	**164.1 %, AUC = 1.00**	**68.6 %, AUC = 0.89**	39.8 %, AUC = 0.76	**62.8 %, AUC = 1.00**
CW-$T_{1\rho}$(1 kHz)	**93.9 %, AUC = 1.00**	59.4 %, AUC = 0.84	4.3 %, AUC = 0.47	31.0 %, AUC = 0.82
CW-$T_{1\rho}$(500 Hz)	**109.7 %, AUC = 0.98**	**64.2 %, AUC = 0.84**	24.4 %, AUC = 0.62	**51.5 %, AUC = 0.96**
CW-$T_{1\rho}$(250 Hz)	**132.3 %, AUC = 0.98**	65.7 %, AUC = 0.78	24.7 %, AUC = 0.64	**56.2 %, AUC = 0.98**
CW-$T_{1\rho}$(125 Hz)	**159.8 %, AUC = 0.91**	52.8 %, AUC = 0.64	39.3 %, AUC = 0.69	**60.8 %, AUC = 0.91**
RAFF	**173.3 %, AUC = 0.89**	54.6 %, AUC = 0.71	60.8 %, AUC = 0.82	**62.7 %, AUC = 1.00**
DE-T_2	**169.3 %, AUC = 1.00**	52.1 %, AUC = 0.80	**87.9 %, AUC = 0.87**	**66.7 %, AUC = 0.98**
T_2	**167.6 %, AUC = 0.98**	43.8 %, AUC = 0.73	78.7 %, AUC = 0.80	**59.9 %, AUC = 0.87**
T_1	**26.2 %, AUC = 0.89**	**22.1 %, AUC = 0.97**	8.2 %, AUC = 0.73	**12.6 %, AUC = 0.87**
$T_{1,Gd}$	−2.00 %, AUC = 0.53	−12.3 %, AUC = 0.62	−10.5 %, AUC = 0.64	−9.8 %, AUC = 0.64
T_{1sat}	**93.6 %, AUC = 1.00**	**67.9 %, AUC = 0.93**	3.8 %, AUC = 0.51	**31.0 %, AUC = 0.87**

$P < 0.05$ in boldface

Table 5

Linear Pearson correlation coefficients between the MRI parameters (full-thickness ROI) and equilibrium modulus (E_{eq}), dynamic modulus (E_{dyn}), water content, optical density (OD, measure of PG content), PI (parallelism index, collagen anisotropy) and OARSI grade, FTIR-derived collagen and PG contents (absorbance of Amide I and Carbohydrate regions). Also, linear Pearson correlation coefficients between the biomechanical parameters (E_{eq} and E_{dyn}) and other reference methods are listed at the bottom of the table.

Parameter (*n* = 14)	**E_{eq}**	**E_{dyn}**	**Water content (%)**	**OD**	**PI**	**OARSI**	**FTIR-Amide I**	**FTIR - Carbohydrate**
$T_{1\rho,Adiab.}$	**−0.80****	**−0.78****	**0.62***	**−0.59***	−0.24	**0.81****	−0.22	−0.32
$T_{2\rho,Adiab.}$	**−0.82****	**−0.71****	0.52	**−0.61***	−0.38	**0.85****	−0.25	−0.50
CW- $T_{1\rho}$, 1.0 kHz	**−0.64***	**−0.68****	0.66	−0.32	−0.30	**0.63***	−0.03	−0.23
CW- $T_{1\rho}$, 500 Hz	**−0.81****	**−0.76****	**0.60***	**−0.60***	−0.28	**0.78****	−0.30	−0.47
CW- $T_{1\rho}$, 250 Hz	**−0.80****	**−0.72****	**0.59***	**−0.59***	−0.32	**0.80****	−0.34	**−0.54***
CW- $T_{1\rho}$, 125 Hz	**−0.67****	**−0.62***	0.48	−0.34	**−0.54***	**0.68****	−0.27	−0.46
RAFF	**−0.74****	**−0.59***	0.40	−0.50	−0.39	**0.74****	−0.37	**−0.54***
DE-T_2	**−0.73****	**−0.57***	0.47	−0.32	**−0.54***	**0.69****	−0.38	**−0.56***
T_2	**−0.65***	−0.49	0.31	−0.24	−0.52	**0.59***	−0.44	**−0.58***
T_1	**−0.71****	**−0.68****	0.45	−0.34	−0.27	**0.64***	**−0.60***	−0.48
T_{1Gd}	0.48	0.52	−0.46	0.45	−0.09	−0.40	0.16	0.28
T_{1sat}	**−0.757****	**−0.806****	**0.57***	**−0.53***	−0.32	**0.80****	−0.42	−0.47
E_{eq}			−0.44	**0.61***	0.36	**−0.90****	0.38	**0.55***
E_{dyn}			**−0.59***	0.46	0.43	**−0.90****	0.31	0.43

* $P < 0.05$

** $P < 0.01$ in boldface